Leukemia (2015) **29,** 356–368

www.nature.com/leu

ORIGINAL ARTICLE

The enzymatic activities of CD38 enhance CLL growth and trafficking: implications for therapeutic targeting

T Vaisitti[1,2], V Audrito[1,2], S Serra[1,2], R Buonincontri[1,2], G Sociali[3], E Mannino[3], A Pagnani[2], A Zucchetto[4], E Tissino[4], C Vitale[5], M Coscia[5], C Usai[6], C Pepper[7], V Gattei[4], S Bruzzone[3] and S Deaglio[1,2]

The ecto-enzyme CD38 is gaining momentum as a novel therapeutic target for patients with hematological malignancies, with several anti-CD38 monoclonal antibodies in clinical trials with promising results. In chronic lymphocytic leukemia (CLL) CD38 is a marker of unfavorable prognosis and a central factor in the pathogenetic network underlying the disease: activation of CD38 regulates genetic pathways involved in proliferation and movement. Here we show that CD38 is enzymatically active in primary CLL cells and that its forced expression increases disease aggressiveness in a xenograft model. The effect is completely lost when using an enzyme-deficient version of CD38 with a single amino-acid mutation. Through the enzymatic conversion of NAD into ADPR (ADP-ribose) and cADPR (cyclic ADP-ribose), CD38 increases cytoplasmic Ca^{2+} concentrations, positively influencing proliferation and signaling mediated via chemokine receptors or integrins. Consistently, inhibition of the enzymatic activities of CD38 using the flavonoid kuromanin blocks CLL chemotaxis, adhesion and *in vivo* homing. In a short-term xenograft model using primary cells, kuromanin treatment traps CLL cells in the blood, thereby increasing responses to chemotherapy. These results suggest that monoclonal antibodies that block the enzymatic activities of CD38 or enzyme inhibitors may prove therapeutically useful.

Leukemia (2015) **29,** 356–368; doi:10.1038/leu.2014.207

INTRODUCTION

CD38 is a surface protein with a wide pattern of expression in cells of hematological and non-hematological origin. It belongs to the family of nucleotide-metabolizing enzymes, a set of molecules involved in the scavenging of extracellular nucleotides (reviewed in Malavasi *et al.*[1]). Besides recycling nucleotides, these enzymes generate compounds that control cellular homeostasis and metabolism. CD38 catalyzes the synthesis of cyclic ADP-ribose (cADPR) a second messenger mobilizing Ca^{2+} from Ryanodine-sensitive stores,[2] and of ADP-ribose (ADPR), which acts as the ligand for the Transient Receptor Potential Melastatin subfamily M type 2 (TRPM2), a receptor-operated membrane Ca^{2+} channel.[3] Moreover, CD38 might, in certain tissues and conditions, catalyze the production of nicotinic acid adenine dinucleotide phosphate, the most potent Ca^{2+}-mobilizing second messenger.[4,5]

The catalytic activity of CD38 is required for various physiological processes, including insulin secretion,[6] muscarinic Ca^{2+} signaling in pancreatic acinar cells,[7] neutrophil chemotaxis,[8] dendritic cell trafficking,[9] oxytocin secretion[10] and in the development of diet-induced obesity.[11]

CD38 is expressed by a number of hematological malignancies, including chronic lymphocytic leukemia (CLL), where it is a negative prognostic marker.[12] CLL is characterized by the expansion of a monoclonal population of mature B cells expressing CD23 and CD5. The clinical behavior is heterogeneous, with some patients requiring early treatment and others remaining stable over a long period of time.[13] Surface expression of CD38 above the clinical cutoff of 20% identifies the subset of CLL patients with a more aggressive variant of the leukemia and a shorter overall survival.[14] Our group has shown that CD38 is a central factor in the pathogenetic network underlying the disease: activation of CD38 regulates genetic pathways involved in proliferation and movement.[15–17] CD38 enhances chemokine responses, adhesion to integrin substrates and matrix metalloprotease activities.[18–21] Together, these functions regulate trafficking of CLL cells to and from thelymph nodes, where microenvironmental conditions favor leukemic growth and survival.[22,23] In CLL cells, CD38 is part of a molecular platform that includes chemokine receptors, integrins and matrix metalloproteases.[24] Here, it integrates signals coming from chemokines and integrins, increasing tyrosine phosphorylation of the key cytoplasmic molecules, including Vav-1 and ERK1/2 (ref. 25). No information is currently available on the molecular mechanisms responsible for these effects.

The hypothesis behind this work is that the enzymatic activities are essential in mediating CD38 functions in CLL cells. The translational relevance of these observations derives from recent reports indicating that monoclonal antibodies targeting CD38 show promising results in clinical trials, at least in myeloma patients.[26–28] If our working hypothesis is confirmed, it would suggest that enzyme inhibitors could be used as therapeutic weapons for targeting CD38.

MATERIALS AND METHODS

Detailed protocols for all sections are described in Supplementary Methods.

[1]Department of Medical Sciences, School of Medicine and Human Genetics Foundation, University of Torino, Torino, Italy; [2]Human Genetics Foundation (HuGeF), Torino, Italy; [3]DIMES-Section of Biochemistry AND CEBR, University of Genova, Genova, Italy; [4]Centro di Riferimento Oncologico (CRO) IRCCS, Aviano, Italy; [5]Division of Hematology, University of Torino, Azienda Universitaria Ospedaliera Città della Salute e della Scienza di Torino, Torino, Italy; [6]Institute of Biophysics, CNR, Genova, Italy and [7]Institute of Cancer & Genetics, Cardiff University, Heath Park, Cardiff, UK. Correspondence: Dr S Deaglio, Department of Medical Sciences, School of Medicine and Human Genetics Foundation, University of Torino, via Nizza, 52, Torino 10126, Italy.
E-mail: silvia.deaglio@unito.it
Received 29 April 2014; revised 20 June 2014; accepted 24 June 2014; accepted article preview online 3 July 2014; advance online publication, 25 July 2014

Cells, mice and reagents

Peripheral blood samples from patients with a confirmed diagnosis of CLL were obtained after informed consent, in accordance with the Institutional Guidelines and the Declaration of Helsinki. Immunocompromised NOD/SCID/γ chain$^{-/-}$ (NSG) mice were from Charles River (Milan, Italy) and were maintained in a pathogen-free animal facility. Mice were treated following the European guidelines and with the approval of the Italian Ministry of Health. Nicotinamide guanine dinucleotide (NGD) and Kuromanin were from Sigma (Milan, Italy), 8-Br-ADPR from Biolog (Bremen, Germany).

Immunofluorescence

The list of antibodies used is in Supplementary Methods. Stained cells were analyzed with a FACSCantoII cytofluorimeter, equipped with the Diva software v8 (BD Biosciences, Milan, Italy).

Generation of Mec-1 transfectants

Mec-1/CD38^{WT}, /CD38^{M} and green-fluorescent protein (GFP) were generated by lentiviral infection and subsequent selection of the CD38^{+} population by using a FACSAria III cell sorter (BD Biosciences).[29] The TRPM2 short-hairpin RNA was from Origene Technologies (Rockville, MD, USA).

Measurement of CD38 enzymatic activities

NADase and cADPR-hydrolase activities were evaluated as described.[30] A fluorimetric assay based on cGDPR generation from NGD was also used, with fluorescence measured using a Synergy Biotek reader (excitation 300 nm, emission 410 nm, BioTek, Winooski, VT, USA).

Determination of intracellular NAD, cADPR and Ca^{2+} concentration

Mec-1 clones (5×10^6) or patient-derived CLL lymphocytes (8×10^6) were lysed (0.3 ml of 0.6 M perchloric acid, 4 °C). NAD and cADPR contents were determined as described[31] and normalized over protein concentration.

To measure $[Ca^{2+}]_i$, cells (2×10^6 cells/ml) were incubated with or without chemokines (10 ng per 10^6 cells, 24 h). Cells were loaded with Fura 2-AM (10 μM, 40 min, 37 °C, Life Technologies, Milan, Italy) and analyzed using a spectrophotometer (Cairn Research Ltd, Faversham, UK). $[Ca^{2+}]_i$ was calculated as in Zocchi *et al.*[32]

Lipid raft isolation

Detergent-insoluble and -soluble membranes were purified by discontinuous sucrose gradient centrifugation, as reported.[18] Of the eight fractions collected from the top, two to four contained the detergent-insoluble membrane and seven to eight the detergent-soluble membrane.

Co-capping experiments

Co-capping experiments were performed using the antibodies described in Supplementary Methods. Cells were analyzed with a TCS SP5 laser scanning confocal microscope equipped with four lasers, images acquired with LAS AF Version Lite 2.4 software (Leica Microsystems, Milan, Italy) and processed with Photoshop (CS6, Adobe Systems, San Jose, CA, USA).

Chemotaxis experiments

Chemotaxis experiments were performed using classical Boyden chamber assays. The migration index (MI) was calculated as described.[18]

Adhesion experiments

Adhesion experiments were performed in 24-well plates coated with recombinant human VCAM-1 (10 mg/ml, R&D Systems, Milan, Italy).[20] Cells were analyzed with a Nikon Eclipse 90i microscope and the ND2 software (Nikon, Tokio, Japan). Staining for phosphorylated Vav-1 was performed as described in Supplementary Methods.

Mouse L cells transfected with human CD31 were used to measure CD38/CD31 interactions. The blocking anti-CD31 antibody Moon-1 was used to interfere with CD38 binding.[33]

MTT assay

MTT assays were performed according to the manufacturer's instructions (Vibrant MTT cell proliferation assay kit, Life Technologies).

In vivo studies and magnetic resonance

Eight-week-old NSG male mice were intraventrally (i.v.) injected with 2.5×10^5 Mec-1 variants in 0.2 ml of phosphate-buffered saline. The animals were weighed twice a week. Tumor growth was checked with magnetic resonance imaging using the Aspect M2 Compact high-performance magnetic resonance imaging imaging system (Aspect Imaging, Toronto, ON, Canada). Peripheral blood, femoral bone marrow and organs (kidneys, liver, spleen, lungs and heart) were analyzed using fluorescence activated cell sorting (FACS) (cells were stained using anti-CD38-Alexa488/-CD19-PE or only -CD19 in Mec-1/GFP^{+}) using the FacsCanto II cytometer and immunohistochemistry to check for infiltrating leukemic cells.

For homing experiments, peripheral blood mononuclear cells (PBMCs) from CLL patients (20×10^6) were i.v. injected in the tail vein of NSG male mice. To inhibit endogenous CD38 activity, 24 and 1 h before injection with the leukemic cells, mice were intraperitoneally injected with 50 mg/kg kuromanin or a vehicle. Human leukemic cells were traced 16 h afterwards as described.[19]

Immunohistochemical analysis

Formalin-fixed, paraffin-embedded sections were stained as described.[34] Antibodies used are described in Supplementary Methods. Slides were analyzed using a DMI3000 optical microscope, equipped with a DCF 310 FX digital camera and images acquired and processed with the LAS AF 3.8 version software (Leica Microsystems). Quantification of staining intensity was performed in ×4 magnification images, using the LAS Application Suite Version 3.8 software (Leica Microsystems) and expressed as percentage of CD20 areas. At least six different areas of the same slide from three independent experiments were analyzed.

Gene expression profiling analysis

In all, 300 ng RNA were amplified and biotinylated using Illumina TotalPrep RNA Amplification Kit (Life Technologies). cRNA (750 ng) was hybridized to HumanHT-12 v4 Expression BeadChips (Illumina, Milan, Italy) using Whole-Genome Expression Direct Hybridisation kit (Illumina) and scanned with iScan System (Illumina). Analysis is described in Supplementary Methods.

Quantitative real-time PCR (qRT-PCR)

RNA samples used for gene expression profiling were converted to cDNA using the High Capacity cDNAReverse Transcription kit (Life Technologies). qRT-PCR was performed using the 7900 HT Fast Real Time PCR system (SDS2.3 software) with commercial primers (TaqMan Gene Expression Assays, Life Technologies, Monza, Italy). The comparative computed tomography method was used to calculate expression relative to the endogenous control.

Statistical analyses

Statistical analyses were performed with GraphPad v6 (GraphPad Software Inc, La Jolla, CA, USA) and are presented as box plots or histograms. In the text, data are presented as mean ± s.e.m. Mann–Whitney or Wilcoxon matched-pairs signed rank test were used to determine statistical significance.

RESULTS

CD38 is enzymatically active in CLL cells

CD38 metabolizes NAD and NADP, generating cADPR, ADPR and nicotinic acid adenine dinucleotide phosphate, all Ca^{2+}-mobilizing compounds. However, the activity of CD38 as a surface enzyme in CLL cells remains unexplored. Purified CD38^{+} and CD38^{-} CLL cells ($n=19$) were analyzed for their ability to produce cGDPR from the NAD analog NGD. Under basal conditions, CD38^{+} cells produced significantly higher levels of cGDPR than their CD38^{-} counterparts (Figure 1a). Consistent with the expression of a functional NAD-metabolizing enzyme, CD38^{+} CLL cells contained lower NAD and higher cADPR levels than CD38^{-} cells (Figure 1b), as expected.[32] The only other enzyme with a similar activity, namely CD157, is not expressed by CLL cells.

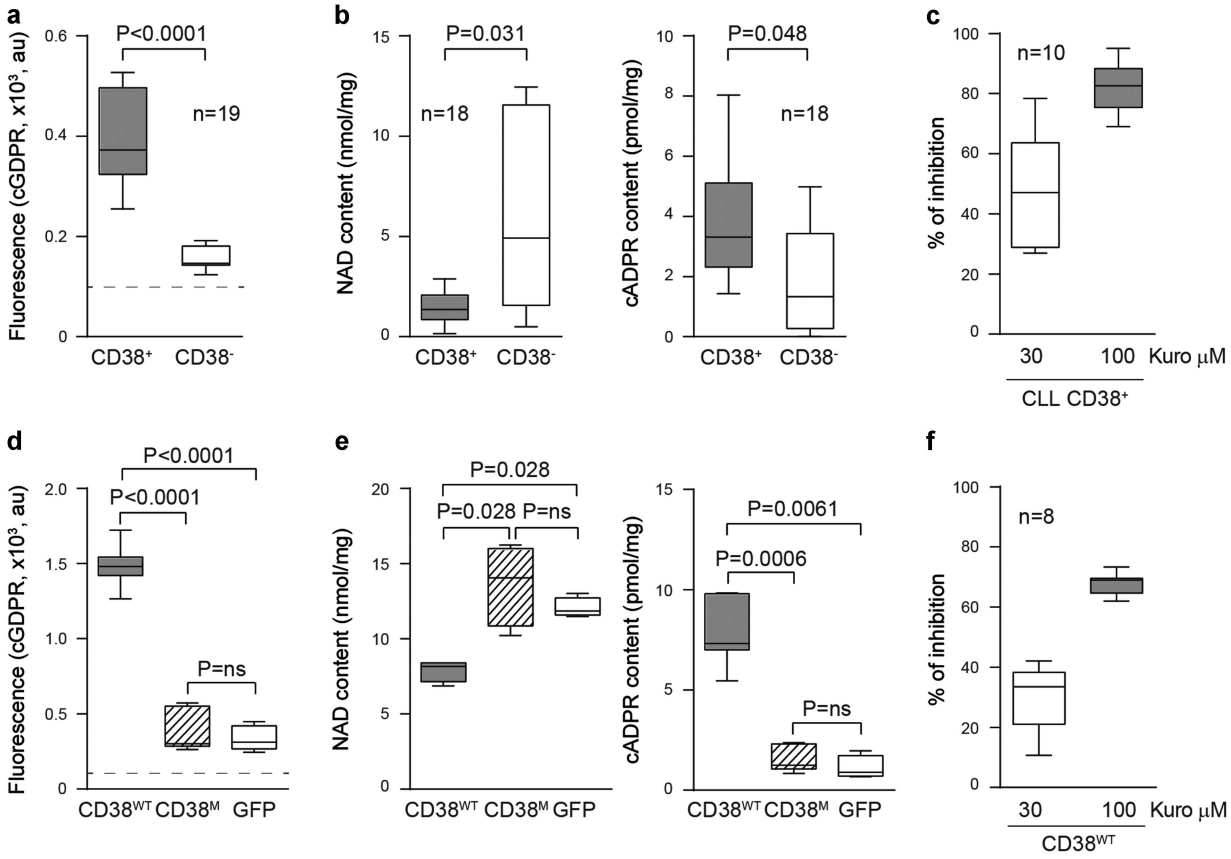

Figure 1. CD38 is enzymatically active in CLL lymphocytes and in a derived cell line model. (**a**) CD38 enzymatic activities were measured in $CD38^+$ (>70% positive cells, $n=9$) and $CD38^-$ (<8% positive cells, $n=10$) CLL cells using NGD as substrate. Accumulation of cGDPR was measured over 180 min. Results are expressed as arbitrary fluorescence units. The dotted line represents fluorescence values without cells. (**b**) NAD and cADPR contents were determined with an enzymatic cycling assay in $CD38^+$ and $CD38^-$ CLL samples ($n=9$). (**c**) $CD38^+$ CLL cells ($n=10$) were pre-incubated with kuromanin (30 or 100 μM, 30 min) before assaying the conversion of NGD into cGDPR over 180 min. Results are expressed as percentage of inhibition. (**d**) Mec-1 cells infected with lentiviruses carrying a wild-type version of CD38 ($CD38^{WT}$), the E226D mutant ($CD38^M$) or GFP were assayed for the production of cGDPR from NGD over 180 min. Results are expressed as in **a**. The dotted line represents fluorescence values without cells. (**e**) NAD and cADPR contents in Mec-1 clones, as measured with an enzymatic cycling assay. (**f**) Percentage of inhibition of the enzymatic activities of CD38 in Mec-1/$CD38^{WT}$ by kuromanin calculated as in **c**.

Recently, flavonoids, such as kuromanin, have been shown to inhibit CD38 enzymatic activities. Among the available molecules, we selected kuromanin because it is active in the low micromolar range, being one of the most potent CD38 inhibitors.[35,36] This was confirmed in CLL cells, where exposure to kuromanin blocked the conversion of NGD to cGDPR in a dose-dependent manner, with a reduction of ~80% when exposing $CD38^+$ CLL cells to 100 μM kuromanin (Figure 1c). Under these conditions, $CD38^+$ CLL cells were indistinguishable from $CD38^-$ ones in terms of NGD degradation (data not shown). As previously reported with other flavonoids of similar activity,[37,38] no cytotoxicity was observed when CLL cells were exposed to 100 μM kuromanin for up to 24 h.

Generation and characterization of Mec-1 clones expressing a wild-type or an enzymatically inactive form of CD38

The CLL-like cell line Mec-1 was used as model to address the functional role of the enzymatic activities of CD38 in the disease. These cells, constitutively $CD38^-$, were infected by lentiviruses carrying the genetic material for a wild-type or an enzymatically inactive form of the molecule ($CD38^{WT}$ and $CD38^M$, respectively). The mutant was generated by introducing a point mutation in the catalytic site (E226D, glutamic acid into aspartic acid), previously shown to be critical for the enzymatic functions.[39] GFP^+ Mec-1 clones (Mec-1/GFP) were generated with the same protocol and used as the control. Three independent clones for each condition were studied. Comparable expression levels of CD38 in the wild-type and the mutant clones were confirmed using RT-PCR, western blot and immunofluorescence staining (Supplementary Figure 1A–C). The mutant form of CD38 was still recognized by the five antibodies used (Supplementary Figure 1C). Mec-1/$CD38^{WT}$ were enzymatically competent, as confirmed using the NGD assay (Figure 1d) and the quantification of NAD glycohydrolase and cADPR hydrolase activities (Supplementary Figure 1D), whereas Mec-1/GFP and /$CD38^M$ cells were unable to metabolize NGD (Figure 1d). In agreement with the results obtained using primary cells, Mec-1/$CD38^{WT}$ cells contained lower NAD and higher cADPR levels, when compared with /$CD38^M$ or /GFP Mec-1 cells (Figure 1e). Enzymatic conversion of NGD was dose-dependently blocked by the addition of kuromanin, with ~70% inhibition using a dose of 100 μM (Figure 1f). Under these conditions, no cytotoxicity was observed.

Mec-1/$CD38^{WT}$ or Mec-1/$CD38^M$ cells exhibit similar CD38 structural organization and signal transduction properties

We first asked whether $CD38^M$ molecules were structurally different from $CD38^{WT}$. Three different observations argue against this hypothesis. First, no differences were observed in the membrane distribution of Mec-1/$CD38^{WT}$ or /$CD38^M$ cells, with ~50% of the protein constitutively localized in detergent-insoluble fractions (Figure 2a), as expected.[40] Second, both

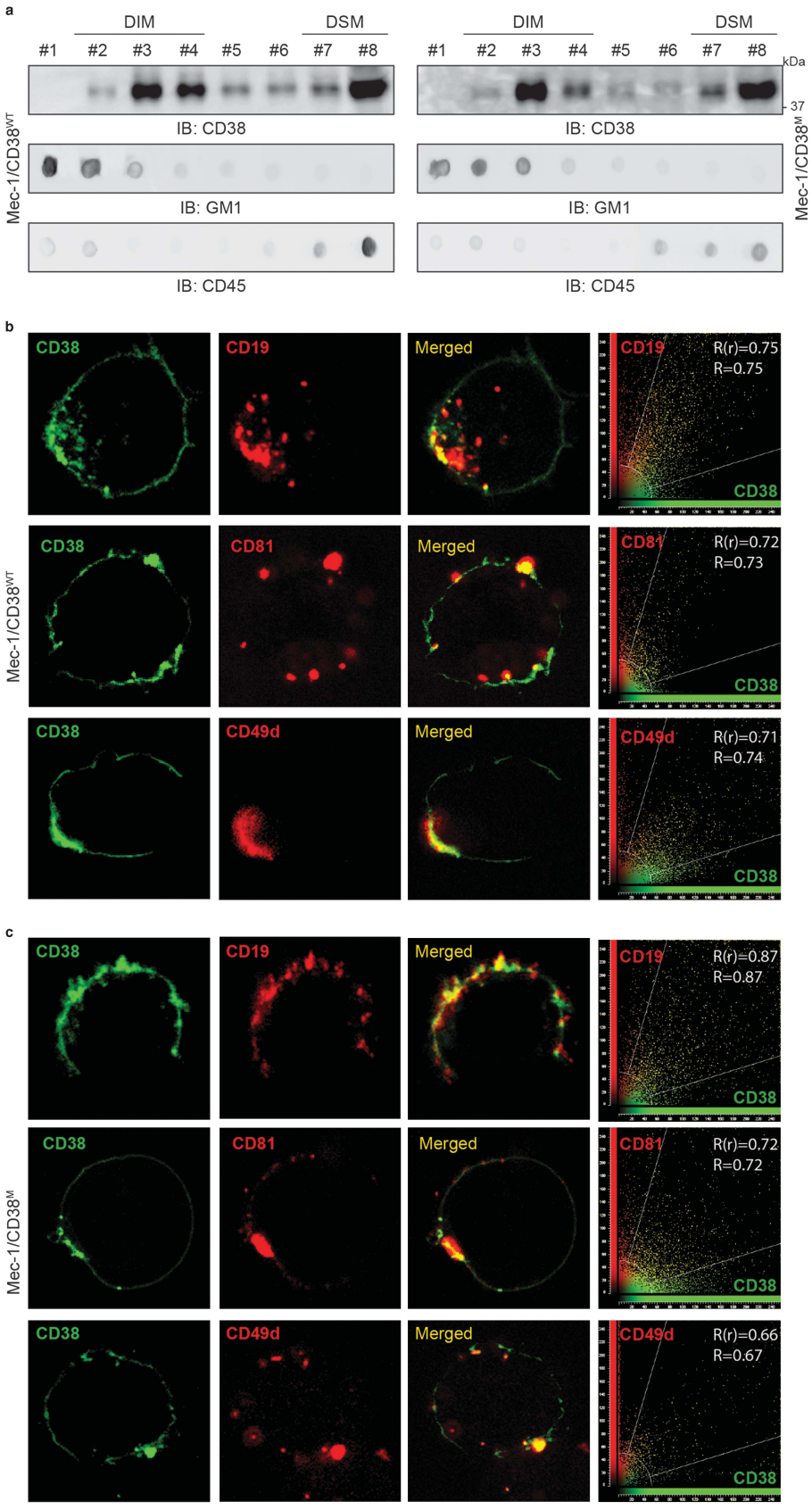

Figure 2. Comparable organization of CD38 molecules in the different Mec-1 clones. (**a**) Membrane fractionation experiments confirm that ~ 50% of CD38 molecules are localized in membrane microdomains, without measurable differences between Mec-1/CD38^{WT} and /CD38^{M} clones. GMI and CD45 were selected as predominantly raft-resident and raft-excluded proteins and used as controls. (**b, c**) Co-capping analyses showing colocalization of CD38 with CD19, CD81 and CD49d, occurring in both Mec-1/CD38^{WT} (**b**) and /CD38^{M} clones (**c**). Scatter plots on the right show cumulative data.

$CD38^{WT}$ and $/CD38^{M}$ molecules were able to associate laterally with other proteins or protein complexes, a known feature of CD38 in different hematopoietic cell lineages.[1] Polar aggregation of $CD38^{WT}$ or $CD38^{M}$ molecules was followed by colocalization of CD19, CD81 and CD49d, with no measurable differences in the two cell lines (Figures 2b and c). Third, cross-linking of CD38 on Mec-1/$CD38^{WT}$ and $/CD38^{M}$ cells with the agonistic IB4 mAb induced a rapid activation of ERK1/2 and p38/Jnk, which peaked at 2 and 10 min, respectively (Supplementary Figures 2A and B), in line with previous findings.[18]

These results indicate that while the single amino-acid mutation in the catalytic site of CD38 completely abrogates the enzymatic activities, it does not alter its structural characteristics.

Mec-1/$CD38^{WT}$ cells show greater chemotactic responses than Mec-1/$CD38^{M}$ or /GFP cells

We then compared the functional properties of the different Mec-1 clones. Mec-1/$CD38^{WT}$ cells were characterized by a higher spontaneous proliferation rate than the $/CD38^{M}$ ($P < 0.0001$) and control/GFP ($P < 0.0001$) cells, as determined with MTT test (Figure 3a). Furthermore, Mec-1/$CD38^{WT}$ migrated significantly more towards CCL19 (mean MI: 14.6 ± 1.7) than Mec-1/$CD38^{M}$ (mean MI: 5.6 ± 1.2) or /GFP cells (mean MI: 6.5 ± 0.8), despite comparable levels of CCR7 receptor expression (Supplementary Figure 3A). Pre-treatment with kuromanin significantly reduced chemotaxis of Mec-1/$CD38^{WT}$ (mean MI: 8.4 ± 1.2, $P < 0.0001$ compared with untreated), whose migration index became comparable to that of Mec-1/$CD38^{M}$ or /GFP clones (Figure 3b). No effects were registered when kuromanin was administered to Mec-1/$CD38^{M}$ or /GFP cells.

In line with previous observations,[41] cultured Mec-1 cells did not respond to CXCL12 or CXCL10 (mean MI towards both chemokines < 1), likely because of low constitutive levels of expression of CXCR4 and CXCR3 receptors (Supplementary Figures 3B and D). The same cells, when examined after 4 weeks of growth in NSG mice, significantly upmodulated both CXCR4 and CXCR3 at the mRNA and protein levels in all the Mec-1 variants (Supplementary Figures 3B and D). Expression of the receptors was followed by a slight increase in chemotactic responses to CXCL12 and CXCL10 in Mec-1/GFP and $/CD38^{M}$ clones. In contrast, Mec-1/$CD38^{WT}$ clones showed a sharp increase in chemotaxis (mean MI towards CXCL12: 28.6 ± 6.2; mean MI towards CXCL10: 25.3 ± 5.3; Figure 3c). Pre-treatment of Mec-1/$CD38^{WT}$ cells with kuromanin (100 μM) significantly reduced chemotaxis to both chemokines (mean MI towards CXCL12: 1.4 ± 0.6; mean MI towards CXCL10: 0.2 ± 0.2). Kuromanin treatment was ineffective in the other two cell lines (Figure 3c).

Mec-1/$CD38^{WT}$ cells show greater adhesion and MMP-9 secretion than Mec-1/$CD38^{M}$ or Mec-1/GFP cells

We then examined the adhesive properties of the different clones on VCAM-1 substrate, selected based on previous findings indicating that CD38 and CD49d (the VCAM-1 receptor) are physically associated in CLL cells and that CD38 increases adhesion to VCAM-1.[20]

A significantly higher number of Mec-1/$CD38^{WT}$ cells (349 ± 41) adhered to VCAM-1, compared with both Mec-1/$CD38^{M}$ (154 ± 39) or /GFP (212 ± 16) cells ($P = 0.001$ and $P = 0.006$, respectively Figure 3d). Phase-contrast microscopy images showed that Mec-1/$CD38^{WT}$ cells bound to VCAM-1 were characterized by filopodia-like protrusions, at variance with both Mec-1/$CD38^{M}$ and /GFP cells, which remained round and loosely attached. Pre-treatment of Mec-1/$CD38^{WT}$ cells with kuromanin significantly compromised adhesion (120 ± 10, $P < 0.0001$ compared with untreated cells), showing similar morphology and adhesion characteristics to Mec-1/$CD38^{M}$ and /GFP cells (Figure 3d).

Lastly, we investigated the ability to digest the extracellular matrix by metalloproteinase 9 (MMP-9), previously shown to be increased in $CD38^{+}$ CLL patients.[21] None of the Mec-1 clones constitutively produced MMP-9; however, after growth in NSG mice, MMP-9 expression was upregulated, with the Mec-1/$CD38^{WT}$ clone producing significantly higher amounts of the enzyme than Mec-1/$CD38^{M}$ or /GFP cells (Figure 3e).

Mec-1/$CD38^{WT}$ clones show elevated $[Ca^{2+}]_i$, chemokine-induced Ca^{2+} responses and signaling in response to chemokines and integrins

A hypothesis to explain the behavioral differences between Mec-1/$CD38^{WT}$ and $/CD38^{M}$ cells is linked to the production of ADPR and cADPR from NAD, which may modulate intracellular Ca^{2+} levels ($[Ca^{2+}]_i$). Consistently, Mec-1/$CD38^{WT}$ cells showed constitutively higher $[Ca^{2+}]_i$ than Mec-1/$CD38^{M}$ (mean $[Ca^{2+}]_i$ in Mec-1/$CD38^{WT}$ 56.6 ± 3.4 versus 34.0 ± 1.4 nM in Mec-1/$CD38^{M}$, $P = 0.03$; Figure 4a). After exposure to CCL19 $[Ca^{2+}]_i$ in Mec-1/$CD38^{WT}$, cells were more than twice that scored by $/CD38^{M}$ cells (mean $[Ca^{2+}]_i$ in Mec-1/$CD38^{WT}$ 174.0 ± 7.0 versus 77.0 ± 2.8 nM in Mec-1/$CD38^{M}$, $P = 0.003$; Figure 4a). The same results were observed when exposing Mec-1/$CD38^{WT}$ and $/CD38^{M}$ immediately after *in vivo* growth to CXCL12 or CXCL10, with Mec-1/$CD38^{WT}$ containing significantly higher $[Ca^{2+}]_i$ under all conditions (Figure 4a). In order to determine whether increased $[Ca^{2+}]_i$ was dependent on the enzymatic activities of CD38, Mec-1/$CD38^{WT}$ cells were incubated with CCL19, in the presence (or absence) of kuromanin, with a complete inhibition of CCL19-induced $[Ca^{2+}]_i$ increase (Figure 4b). By interfering with TRPM2 function using 8-Br-ADPR, a TRPM2 antagonist,[42,43] the CCL19-induced increase in $[Ca^{2+}]_i$ was abrogated (Figure 4b). Similar results were obtained after stable silencing of TRPM2 in Mec-1/$CD38^{WT}$. The specificity of this effect was shown by infection of Mec-1/$CD38^{WT}$ with a scramble short-hairpin RNA, which did not affect CCL19 responses (Figure 4b). These findings suggest that ADPR-mediated Ca^{2+} entry from the extracellular compartment is initially involved in activating chemotaxis.

Increased $[Ca^{2+}]_i$ correlated with enhanced signal transduction activated by chemokines or by integrins: Mec-1/$CD38^{WT}$ cells were characterized by higher and more durable phosphorylation of ERK1/2 and p38/Jnk in response to CXCL12 than either $/CD38^{M}$ or /GFP cells (Figure 4c). Similar results were obtained when studying phosphorylation of Vav-1, an early event in the downstream pathway leading to actin polymerization and cytoskeleton polarization.[20,44] Mec-1/$CD38^{WT}$ cells showed increased Vav-1

Figure 3. Mec-1/$CD38^{WT}$ cells show enhanced proliferation, chemotaxis, adhesion and MMP-9 production. (**a**) Box plot showing cumulative results ($n = 8$) of MTT assays comparing Mec-1/$CD38^{WT}$, $/CD38^{M}$ and /GFP cells. (**b, c**) Box plots showing cumulative results of chemotaxis experiments performed using CCL19 (**b**), CXCL12 and CXCL10 (**c**) as attractants. Experiments in **b** were performed using Mec-1 clones grown *in vitro*, whereas those in **c** were performed using the same cells *ex vivo*. Where indicated Mec-1/$CD38^{WT}$ cells were pre-incubated with kuromanin (100 μM for 30 min) to inhibit CD38 enzymatic activities. (**d**) Cumulative results of adhesion experiments of the different Mec-1 variants on recombinant human VCAM-1. The mean number of adherent cells/field was obtained by counting six different fields/slide of at least three independent experiments. The images on the right show representative morphological changes of the Mec-1 variants. (**e**) Gelatin zymography assays showing MMP-9 activity in Mec-1/$CD38^{WT}$, $/CD38^{M}$ and /GFP cells *ex vivo*. The representative image on the right shows that the same cells cultured *in vitro* do not produce MMP-9.

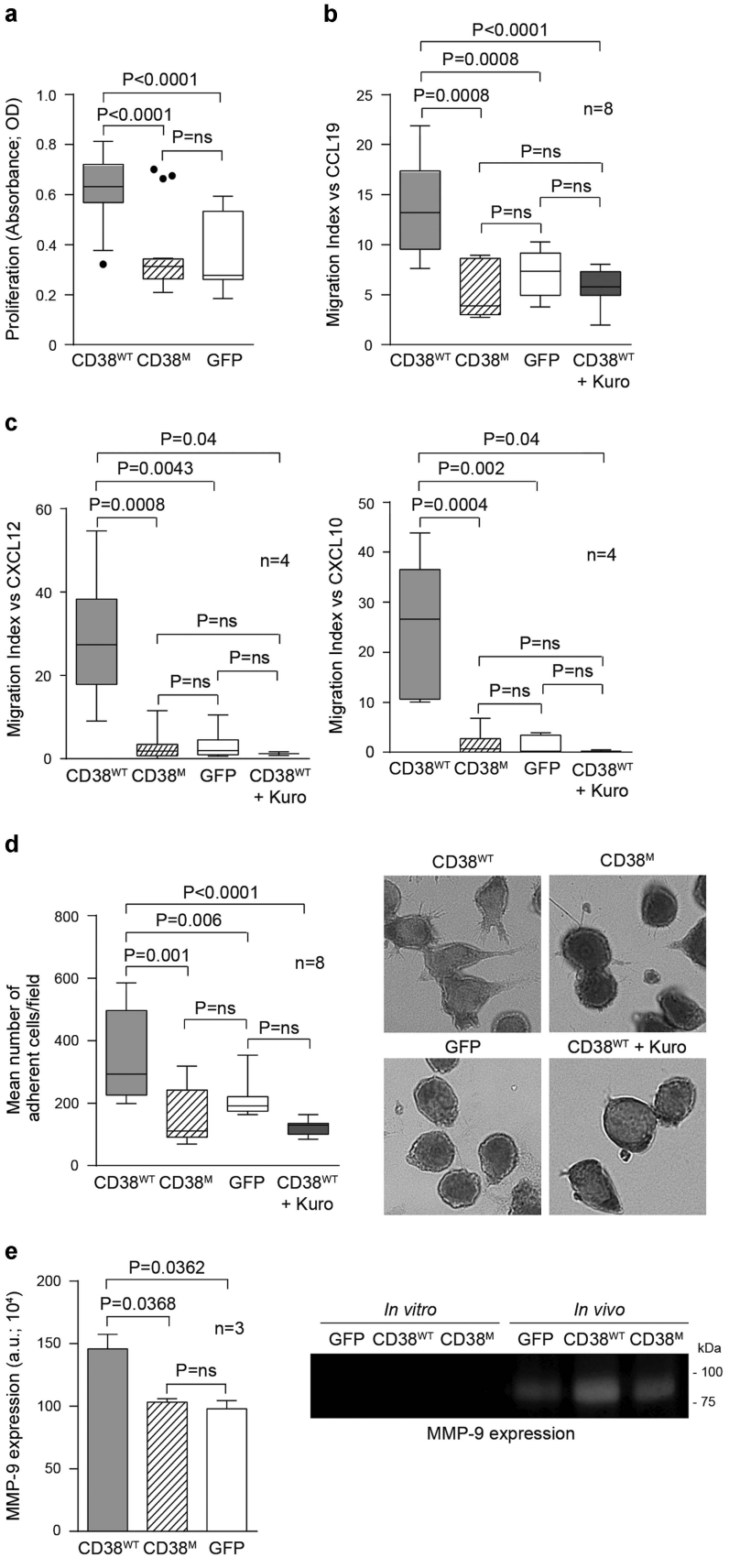

activation and concentration of the phosphorylated form at the adhesion sites. Pre-treatment of these cells with kuromanin reduced Vav-1 phosphorylation to the levels scored by Mec-1/GFP or /CD38^{M} cells (Figure 4d).

Only Mec-1/CD38^{WT} cells bind the CD31 non-substrate ligand

CD31 is the non-substrate ligand for CD38 (ref. 33): CD38/CD31 interactions activate signaling pathways modulating growth and motility of CLL cells.[17] CD31 may be expressed by CLL cells and it is also present at low density in Mec-1 cells, with no differences among the different variants.[45] To measure CD38–CD31 binding on opposing cells, Mec-1 clones were interacted with mouse L-cells transfected with human CD31 (L-CD31^{+}) or control mock-transfected cells (L-mock) under dynamic conditions that minimize integrin activation. Mec-1/CD38^{WT} were the only cells that stably bound to L-CD31^{+}, whereas no significant interaction could be stabilized using L-mock cells ($P < 0.0001$, Figure 4e). Consistent with this finding, pre-incubation of L-CD31^{+} cells with Moon-1, an anti-CD31 monoclonal antibody (mAb) that binds the domain involved in the interaction with CD38, completely abrogated binding (Figure 4e), confirming that the interaction is specific. The use of kuromanin and of 8-Br-ADPR was followed by a significant decrease in CD31 binding ($P < 0.0001$ and $P = 0.002$, respectively, compared with untreated cells), suggesting that Ca^{2+} fluxes mediated by TRPM2 in Mec-1/CD38^{WT} cells are critical in the molecule's adhesion to the non-substrate ligand (Figure 4e). This finding is in keeping with independent observations suggesting that CD38 may function as an active enzyme once its tridimensional structure is stabilized through interactions with other proteins.[46]

Mec-1/CD38^{WT} cells are more aggressive than Mec-1/CD38^{M} or Mec-1/GFP cells using xenograft models

To compare the *in vivo* behavior of the different Mec-1 variants, Mec-1/CD38^{WT}, /CD38^{M} and /GFP cells (0.25×10 (ref. 6)) were injected into the tail vein of NSG mice and left to engraft. This is considered to be a reproducible model of aggressive CLL that develops rapidly, allows measurements of tumor growth and may be exploited as a therapeutic testing model.[47]

All Mec-1 clones showed complete engraftment efficiency. However, Kaplan–Meier survival curves indicated that mice injected with Mec-1/CD38^{WT} cells were characterized by significantly shorter survival (median of 30 days) when compared with those injected with Mec-1/GFP (median of 35.5 days, $P = 0.0024$) and Mec-1/CD38^{M} cells (median of 36 days, $P = 0.0017$; Figure 5a). These experiments were repeated using cells from three independent clones with overlapping results.

The greater aggressiveness of Mec-1/CD38^{WT} cells as compared with the other two variants was confirmed in a set of experiments where mice were analyzed after 25 days. Animals xenografted with Mec-1/CD38^{WT} cells lost more weight than those injected with Mec-1/GFP or Mec-1/CD38^{M} cells ($P = 0.001$ and $P = 0.026$, respectively, Figure 5b). In agreement with previous data showing that Mec-1 home preferentially to the kidney,[47] all animals showed extensive colonization of the kidneys by leukemic cells and eventually died of renal failure. However, on day 25 the Mec-1/CD38^{WT} group invariably presented with more heavily infiltrated kidneys than the other two sets of animals (Figures 5c and d). Magnetic resonance imaging after 21 days highlighted massive lesions in these organs in mice xenografted with Mec-1/CD38^{WT} cells, whereas the other animals showed minimal involvement (Figure 5e). Immunohistochemical analysis confirmed the higher number of Mec-1/CD38^{WT} cells compared with the other clones (Figure 5f). Increased metastatic lesions in the Mec-1/CD38^{WT} group were also highlighted in the liver, lungs and bone marrow, as indicated by staining with anti-human CD20 mAb (Supplementary Figures 4A and B). CD38 expression *in vivo* was maintained by both Mec-1/CD38^{WT} and /CD38^{M} clones throughout the experiment, as determined using immunohistochemistry and FACS analyses (Supplementary Figures 4C and D).

These results indicate that the presence of an enzymatically functional CD38 is sufficient to increase disease aggressiveness and that this phenotype is lost in the presence of an enzymatically inactive variant of the molecule.

Mec-1/CD38^{WT} cells show a distinct gene signature

Gene expression profiling was then used to characterize the signature of Mec-1/CD38^{WT} and Mec-1/CD38^{M} following subtraction of the background values of Mec-1/GFP (Figure 6a). Transcriptome profiling was performed using cells *in vitro* and *in vivo*: in both cases Mec-1/CD38^{WT} were clearly distinct in an unsupervised hierarchical analysis (Supplementary Figure 5A). Mec-1/CD38^{WT} showed 2514 differentially expressed genes (Supplementary Figure 5A). Among them, 1991 (79%) were selectively modulated in the *in vivo* mouse model, whereas 385 sequences characterized the *in vitro* signature and 138 were common to both (Figure 6a). Interrogation of the 2514 differentially expressed genes using functional online annotation tools confirmed enrichment for biological processes including signal transduction (27%), cell adhesion (14%), chemokine signaling, cytokine–cytokine receptor interactions (11%), proliferation (10%) and leukocyte transendothelial migration (5%; Supplementary Figure 5B). This signature was already evident when analyzing the 138 'common' genes. However, the absolute number of genes belonging to these categories and their *P*-values increased significantly in the *in vivo* versus *in vitro* comparison (Figures 6b and c), suggesting that these pathways are enhanced once the cells grow in mice. Quantitative RT-PCR analysis of selected genes (CXCL10, IL-18RAP and IL-10) was used to validate data, confirming a direct correlation between microarray and qRT-PCR data ($R^2 = 0.79$, $P < 0.0001$, Supplementary Figures 5C and F). Gene expression profiling provided genome-wide confirmation of the functional data obtained *in vitro*.

Figure 4. Mec-1/CD38^{WT} clones show elevated $[Ca^{2+}]_i$, signaling in response to chemokines and integrins and are the only ones to bind the CD31 ligand. (**a**) Measurement of $[Ca^{2+}]_i$ in Fura-2-loaded Mec-1/CD38^{WT} and Mec-1/CD38^{M} cells, by spectrophotometric assays under basal conditions and after CCL19, CXCL12 and CXCL10 treatment. (**b**) The same experiments were performed using Mec-1/CD38^{WT} cells pre-treated with kuromanin or Mec-1/CD38^{WT} infected with an shTRPM2 or a scramble short-hairpin RNA lentiviruses and exposed to CCL19. For all experiments, chemokines were used at 10 ng per 10^6 cells for 24 h. (**c**) Mec-1/CD38^{WT} show enhanced CXCL12 signaling. The different Mec-1 variants were treated with CXCL12 (10 ng per 10^6 cells), lysed and analyzed for the activation of ERK1/2 and p38/JNK. (**d**) The different Mec-1 variants were left to adhere on VCAM-1-coated plates before washing, fixing and staining with anti-pVav-1 followed by TRITC-conjugated secondary antibody (red) and Alexa633 phalloidin (green). Red fluorescence intensity is quantified on the right. (**e**) Adhesion assay measuring binding of Mec-1/CD38^{WT}, /CD38^{M} or /GFP cells on L-CD31^{+} cells in the presence or absence of the anti-CD31 monoclonal antibody Moon-1. L-mock fibroblasts were used as control. Adhesion of Mec-1/CD38^{WT} was also measured after pre-treatment with kuromanin or 8-Br-ADPR. Mec-1 cells were labeled with calcein-AM and interacted with adherent fibroblasts (60 min, 4 °C, dynamic conditions). Results are expressed as arbitrary units of fluorescence intensity.

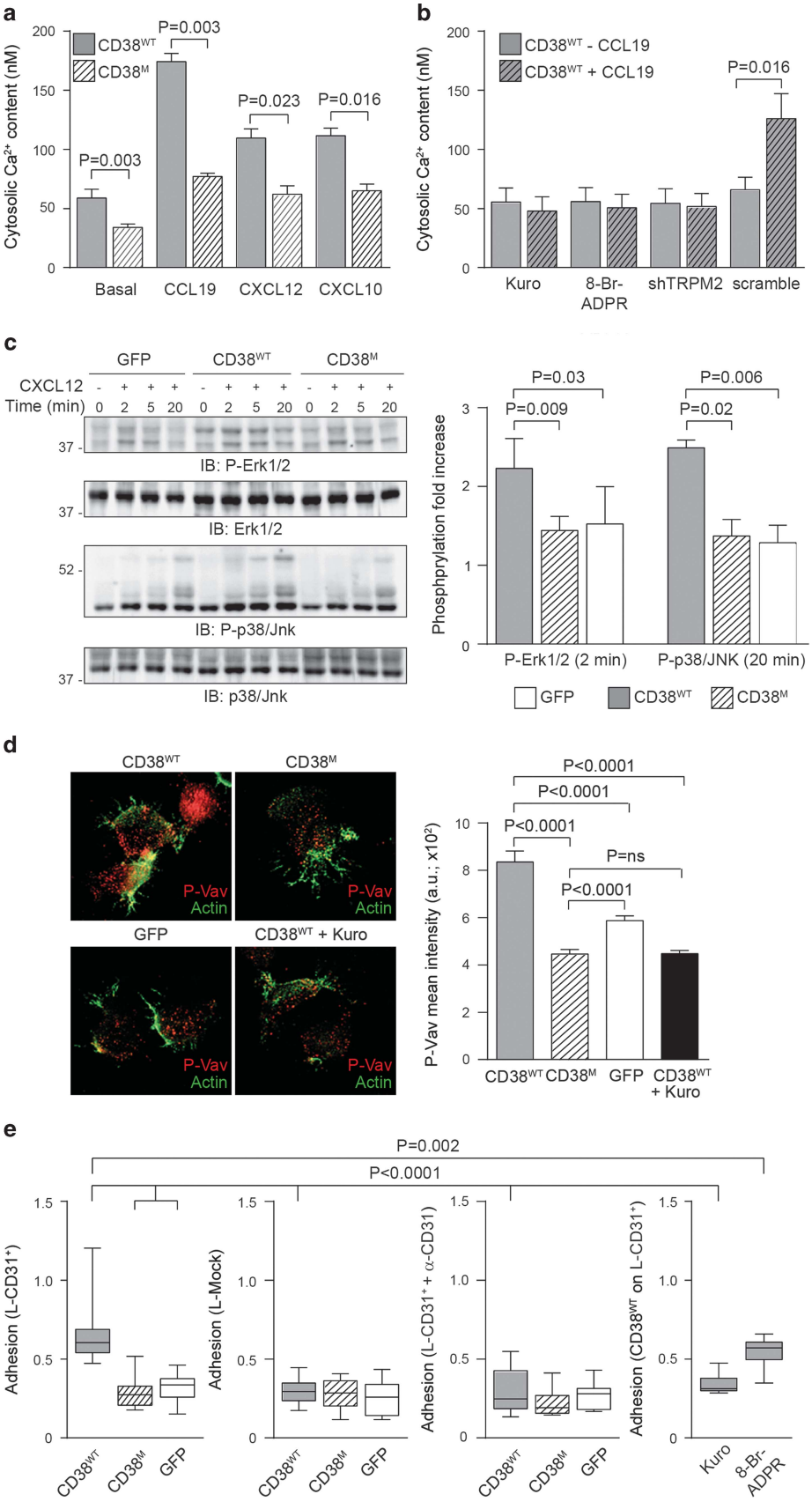

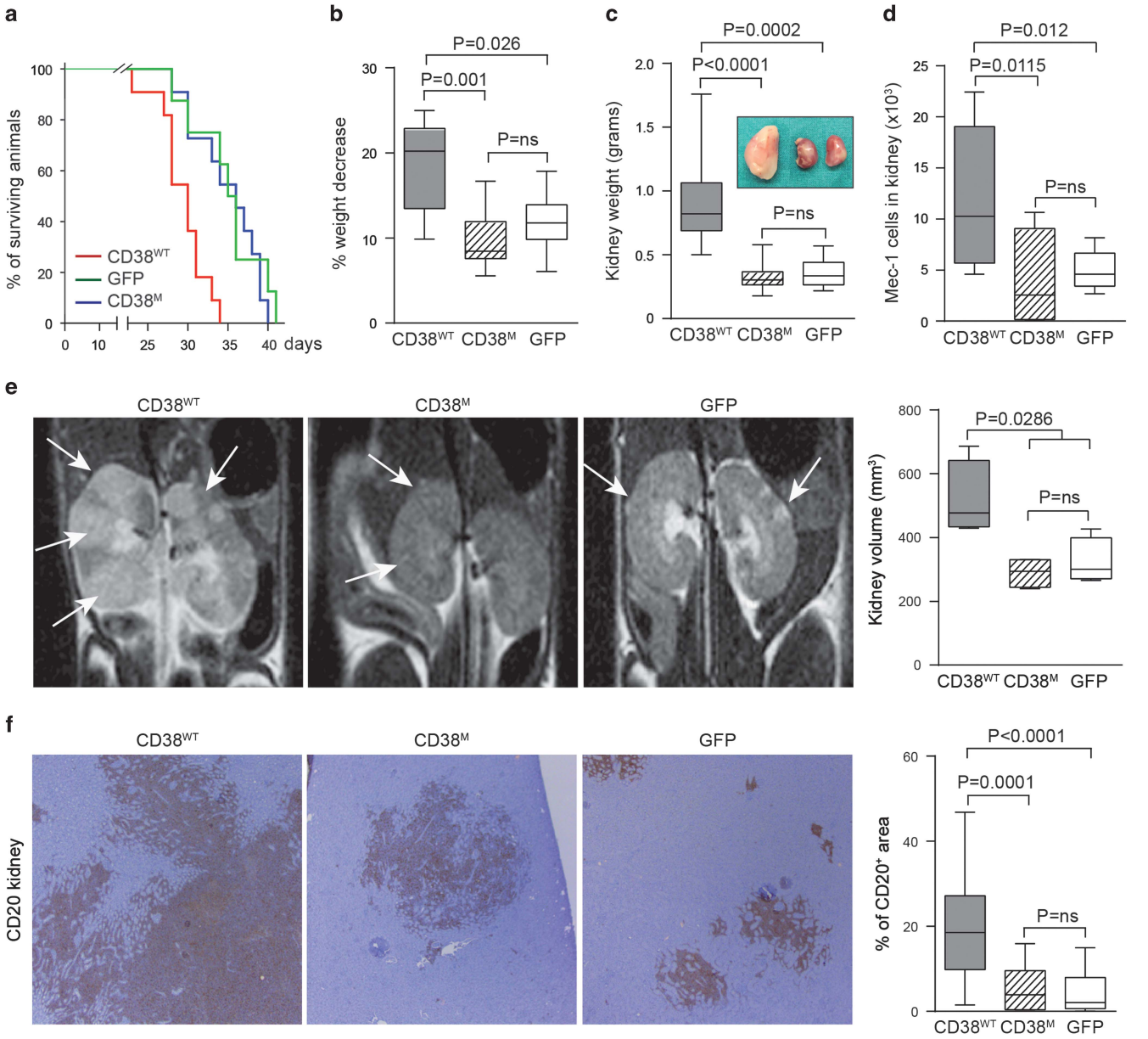

Figure 5. The enzymatic activities of CD38 increase Mec-1 cell aggressiveness in a xenograft model. (**a**) Kaplan–Meier curves showing survival of NSG mice xenografted with Mec-1/CD38^{WT}, /CD38^{M} or /GFP cells (0.25×10^6 i.v.). (**b**) Box plot showing the percentage of weight decrease or (**c**) of weight of the right kidney in NSG mice xenografted with Mec-1 cells and evaluated on day 25. At least eight animals under each condition were evaluated. (**c**) Representative images of the kidneys. (**d**) Measurement of tumor infiltration with flow cytometry of minced kidney preparations (5×10^5 events/sample, eight independent experiments/group) stained with anti-human CD19-PE and anti-human-CD38-Alexa488 (except for control Mec-1/GFP cells where only anti-CD19-PE was used). (**e**) Magnetic resonance imaging (MRI) of the kidneys of representative mice injected with Mec-1/CD38^{WT}, /CD38^{M} or /GFP cells and analyzed after 21 days. Arrows indicate metastatic sites. Box plot on the right shows cumulative data from eight animals per group. (**f**) Low-magnification images of kidney sections stained using an anti-CD20 antibody. Box plot on the right shows cumulative data derived from the analysis of eight sections from eight animals/group.

Proof-of-principle of the therapeutic potential of inhibitors of the enzymatic activity of CD38

A short-term xenograft model based on injection of patient-derived lymphocytes was then used to test the potential of enzymatic inhibitors of CD38 as therapeutics. NSG mice were pre-treated with kuromanin to reduce the activity of endogenous CD38 (Supplementary Figure 6), with no evident toxicity, as inferred from the microscopic analysis of parenchymatous organs. PBMCs from CLL patients were then treated with kuromanin before i.v. injection into NSG mice. Homing to the spleen and BM was measured using flow cytometry after 16 h. Kuromanin exposure significantly prevented homing to the spleen and to the BM (Figure 7a), keeping CLL cells in the blood, where they could still be traced in significantly higher numbers than under untreated conditions (mean number of circulating CD38$^+$ CLL cells: $11\,074 \pm 2846$ in the untreated condition versus $34\,406 \pm 9545$ following kuromanin treatment, $P = 0.0039$, Figure 7a).

These experiments suggest that kuromanin blocks extravasation of CLL lymphocytes, keeping them in the blood, where they may be more susceptible to conventional or novel drugs. Even if homing to the spleen could also be due to passive mechanisms and not only to active extravasation,[48] it should be noted that cells remaining in the blood did not show signs of apoptosis. To prove this point, NSG mice were xenografted with Mec-1/CD38^{WT} cells

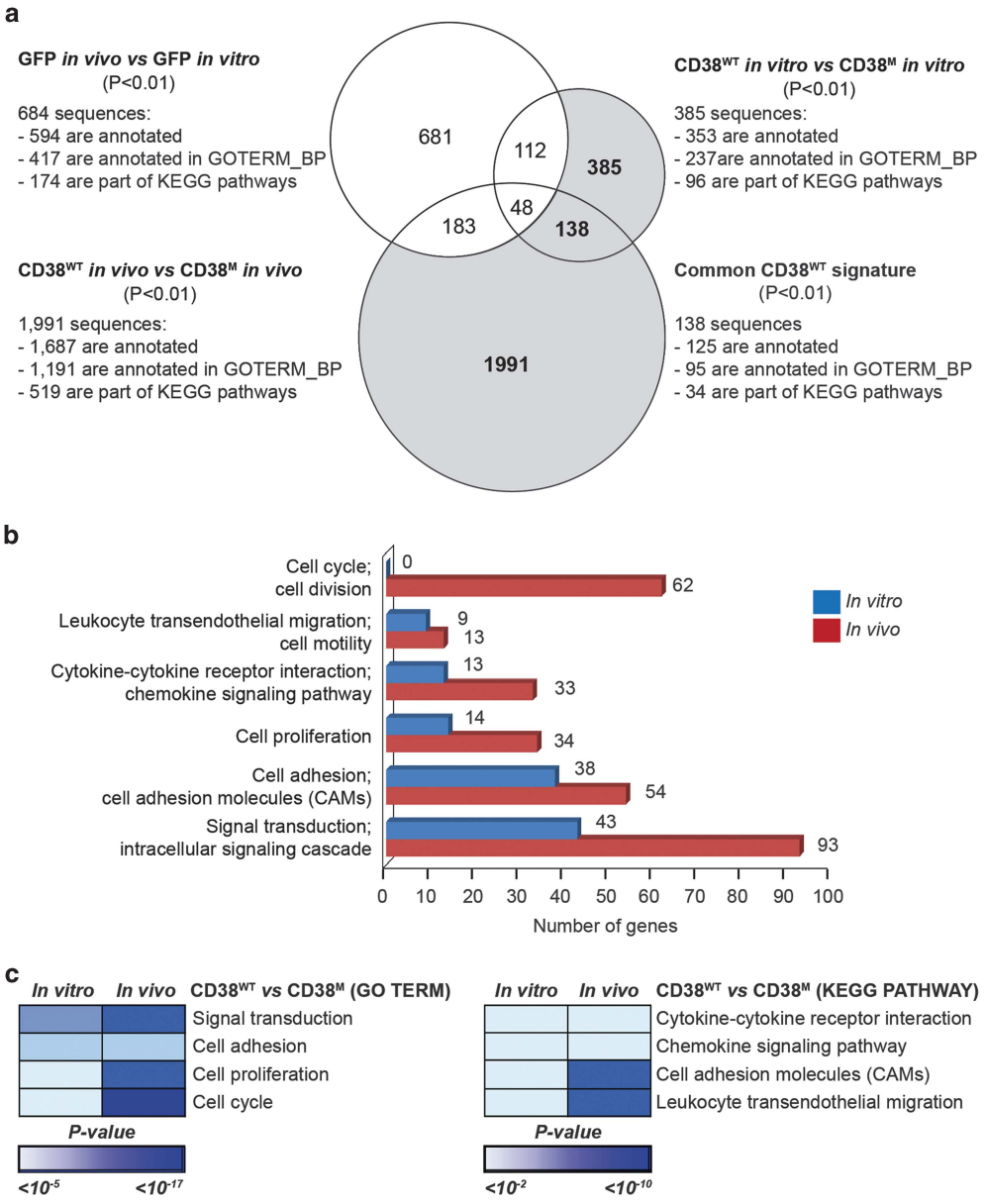

Figure 6. Identification of a Mec-1/CD38^{WT} gene expression signature. (**a**) Venn diagrams showing the strategy chosen to identify the Mec-1/CD38^{WT} signature. (**b**) Pathway enrichment analysis of sequences characterizing Mec-1/CD38^{WT} cells *in vitro* (blue bars) and *in vivo* (red bars). The numbers indicate the absolute number of genes belonging to each pathway. (**c**) Differentially modulated GO terms and KEGG pathways obtained by comparing Mec-1/CD38^{WT} and /CD38^{M} cells *in vitro* or after *in vivo* growth.

and treated with fludarabine, kuromanin or their combination after 10 days. Results indicate that the animals receiving kuromanin and fludarabine showed diminished metastatic colonization in the liver (% of CD19^{+}/CD38^{+} cells: 29.6 ± 3.5 untreated versus 10.2 ± 0.9 kuromanin versus 8.9 ± 1.8 fludarabine versus 4.5 ± 0.9 kuromanin and fludarabine, Figure 7b) and increased levels of cell death in Mec-1/CD38^{WT} found in the right kidney (% of apoptotic/necrotic cells: 16.1 ± 1.4 untreated versus 22.0 ± 2.5 kuromanin versus 25.1 ± 3.1 fludarabine versus 36.9 ± 4.2 kuromanin and fludarabine, Figure 7c) than when each drug was administered alone.

These results confirm that CD38 is directly involved via its enzymatic activities in determining a more aggressive clinical course of CLL. Consequently, inhibitors of CD38 enzymatic activities may be therapeutically relevant.

DISCUSSION

From a basic science perspective, the results of this work indicate that the enzymatic activities of CD38 are essential in regulating CLL growth and trafficking. This conclusion is based on the comparative analysis of CLL-derived cell line clones expressing a wild-type or mutant form of CD38. Mec-1/CD38^{WT} cells proliferate more and show enhanced chemotaxis, adhesion and MMP-9 secretion, three essential steps in the homing process. When xenografted in NSG mice, Mec-1/CD38^{WT} grow faster and show increased colonization of target organs as compared with /CD38^{M} or control cells. These results are in keeping with the hypothesis that CD38 directly contributes to disease aggressiveness and suggest that the enzymatic activities are essential in determining the phenotype. As an indirect proof of the relevance of the enzymatic activities of CD38 in modulating growth and movement

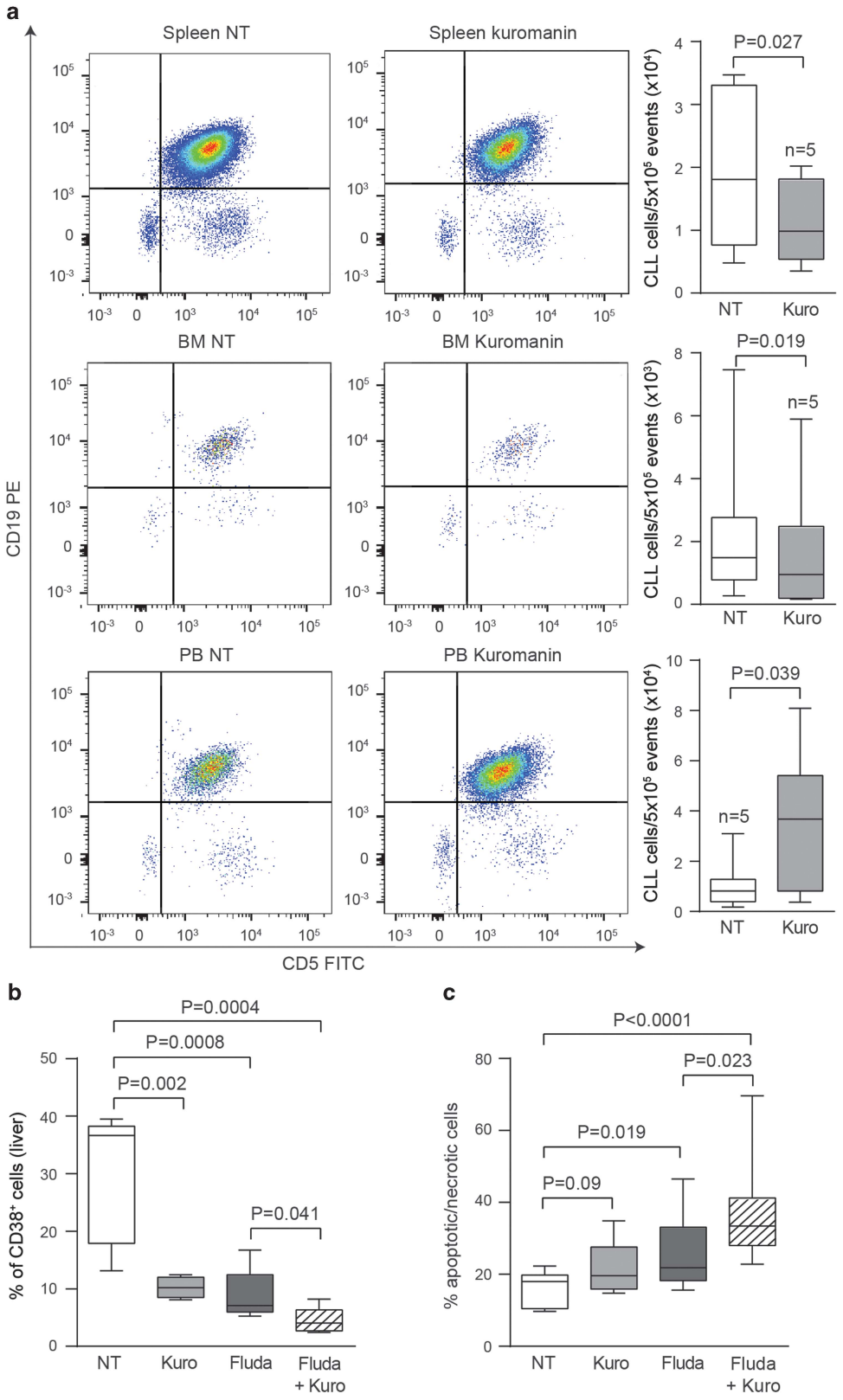

Figure 7. Proof-of-principle of the therapeutic potential of inhibitors of the enzymatic activity of CD38. (**a**) PBMCs from CLL patients were pre-treated with kuromanin before injection in NSG mice. Endogenous CD38 activity was reduced by pre-treatment of the animals (24 h before) with kuromanin. Dot plots represent cells stained with anti-CD19 and -CD5, after gating for SSC and CD45. Box plots on the right show cumulative data from five patients. (**b**) Percentage of Mec-1/CD38^{WT} recovered from the right lobe of the liver in NSG mice treated with kuromanin, fludarabine or their combination. (**c**) Box plot indicating the percentage of apoptotic/necrotic Mec-1/CD38^{WT} cells in the kidneys of mice treated with kuromanin, fludarabine or their combination.

of leukemic cells, the selective inhibitor kuromanin completely abrogated the advantage of Mec-1/CD38^{WT} cells both in *in vitro* and *in vivo* assays. Even if this molecule did not show toxicity in the *in vitro* or *in vivo* setting, other effects besides the inhibition of CD38 enzymatic activities cannot be ruled out.

The different behavior of Mec-1/CD38^{WT} cells could not be explained by differences in the molecular organization of CD38 on the membrane. Binding of the five monoclonal antibodies tested, localization in lipid rafts and lateral associations with different proteins were maintained in Mec-1/CD38^{M} cells. Furthermore, CD38 ligation with agonistic antibodies triggered activation of a signaling pathway in both cell lines, suggesting that the mutation does not significantly affect the structural properties of the molecule.

The two main features that distinguished Mec-1/CD38^{WT} from /CD38^{M} were a different regulation of $[Ca^{2+}]_i$ and the ability to bind the CD31 ligand. Increased $[Ca^{2+}]_i$ may be explained on the basis of the enzymatic conversion of NAD into Ca^{2+}-active compounds, cADPR and ADPR. This phenomenon is evident under basal conditions, with Mec-1/CD38^{WT} cells having higher $[Ca^{2+}]_i$, in line with previous reports.[32] Importantly, Mec-1/CD38^{WT} cells also showed a higher increase in $[Ca^{2+}]_i$ in response to chemokines. In each condition, $[Ca^{2+}]_i$ of Mec-1/CD38^{WT} was at least double that of /CD38^{M} or control cells. TRPM2, a membrane channel that is modulated by ADPR,[3] was the key Ca^{2+} channel mediating increased $[Ca^{2+}]_i$ under basal and under stimulated conditions. This conclusion was inferred by using pharmacological inhibitors or gene silencing. The role of cADPR, which was found in higher amounts in Mec-1/CD38^{WT}, may be linked to increased Ca^{2+} responses through two different mechanisms. On one side, it could synergize with ADPR to potentiate TRPM2 activation,[49] whereas on the other it could trigger a calcium-induced calcium-release mechanism from Ryanodine-sensitive stores.[2]

The second element distinguishing Mec-1/CD38^{WT} from /CD38^{M} cells was the ability to bind the CD31 ligand, which was lost when the enzymatic activity was disrupted. This information is consistent with data from crystallography studies that indicate that CD31 binding could be a prerequisite for the stabilization of dimers or multimers of CD38, which are the only active forms of the enzyme.[50]

The relevance of these results in CLL biology was first confirmed by the finding that CD38 is enzymatically active. Second, inhibition of CD38 using kuromanin in patient-derived CLL cells significantly compromised CXCL12-mediated chemotaxis (Supplementary Figure 7). Third, homing of CLL cells from the blood to lymphoid organs was significantly prevented in mice treated with kuromanin, confirming that these effects are also relevant *in vivo*.

From the translational point of view, the results of this work provide a proof-of-principle that inhibitors of the enzymatic activities of CD38 could have therapeutic potential.[51] So far, the only CD38-targeting drugs that have reached the clinic are mAbs.[52,53] Their effects are mostly based on the ability of the Fc portion of the molecule to trigger antibody-dependent cellular cytotoxicity or complement-dependent cytotoxicity. Our results indicate that drugs interfering with the core functions of CD38 would limit proliferation of leukemic cells, as well as their access to growth-privileged sites. The preparation of antibody fractions, peptides or aptamers that can block CD38 enzymatic activities with high affinity and specificity of action is likely to provide the medical community with novel therapeutic weapons for CLL, as well as for patients with other hematological malignancies.

CONFLICT OF INTEREST

The authors declare no conflict of interest.

ACKNOWLEDGEMENTS

We thank M Lamusta and K Gizzi for excellent technical support. This work is dedicated to the memory of Christian Usseglio Mattiet. This work is supported by grants from the Italian Ministries of Education, University and Research (Futuro in Ricerca 2008 no. RBFR08ATLH and 2012 no. RBFR12D1CB, PRIN 2009 no. 2009LMEEEH_002), the Italian Ministry of Health (Bando Giovani Ricercatori 2008 no. GR-2008-1138053, GR-2010-2317594 and GR-2011-02349282), the Associazione Italiana per la Ricerca sul Cancro Foundation (IG 12754) and Cariplo Foundation (grant #2012-0689).

REFERENCES

1 Malavasi F, Deaglio S, Funaro A, Ferrero E, Horenstein AL, Ortolan E *et al.* Evolution and function of the ADP ribosyl cyclase/CD38 gene family in physiology and pathology. *Physiol Rev* 2008; **88**: 841–886.
2 Lee HC. Cyclic ADP-ribose and nicotinic acid adenine dinucleotide phosphate (NAADP) as messengers for calcium mobilization. *J Biol Chem* 2012; **287**: 31633–31640.
3 Perraud AL, Fleig A, Dunn CA, Bagley LA, Launay P, Schmitz C *et al.* ADP-ribose gating of the calcium-permeable LTRPC2 channel revealed by Nudix motif homology. *Nature* 2001; **411**: 595–599.
4 Cosker F, Cheviron N, Yamasaki M, Menteyne A, Lund FE, Moutin MJ *et al.* The ecto-enzyme CD38 is a nicotinic acid adenine dinucleotide phosphate (NAADP) synthase that couples receptor activation to Ca2+ mobilization from lysosomes in pancreatic acinar cells. *J Biol Chem* 2010; **285**: 38251–38259.
5 Schmid F, Fliegert R, Westphal T, Bauche A, Guse AH. Nicotinic acid adenine dinucleotide phosphate (NAADP) degradation by alkaline phosphatase. *J Biol Chem* 2012; **287**: 32525–32534.
6 Okamoto H, Takasawa S, Nata K. The CD38-cyclic ADP-ribose signalling system in insulin secretion: molecular basis and clinical implications. *Diabetologia* 1997; **40**: 1485–1491.
7 Fukushi Y, Kato I, Takasawa S, Sasaki T, Ong BH, Sato M *et al.* Identification of cyclic ADP-ribose-dependent mechanisms in pancreatic muscarinic Ca(2+) signaling using CD38 knockout mice. *J Biol Chem* 2001; **276**: 649–655.
8 Partida-Sanchez S, Cockayne DA, Monard S, Jacobson EL, Oppenheimer N, Garvy B *et al.* Cyclic ADP-ribose production by CD38 regulates intracellular calcium release, extracellular calcium influx and chemotaxis in neutrophils and is required for bacterial clearance *in vivo*. *Nat Med* 2001; **7**: 1209–1216.
9 Partida-Sanchez S, Goodrich S, Kusser K, Oppenheimer N, Randall TD, Lund FE. Regulation of dendritic cell trafficking by the ADP-ribosyl cyclase CD38: impact on the development of humoral immunity. *Immunity* 2004; **20**: 279–291.
10 Jin D, Liu HX, Hirai H, Torashima T, Nagai T, Lopatina O *et al.* CD38 is critical for social behaviour by regulating oxytocin secretion. *Nature* 2007; **446**: 41–45.
11 Aksoy P, Escande C, White TA, Thompson M, Soares S, Benech JC *et al.* Regulation of SIRT 1 mediated NAD dependent deacetylation: a novel role for the multifunctional enzyme CD38. *Biochem Biophys Res Commun* 2006; **349**: 353–359.
12 Deaglio S, Vaisitti T, Aydin S, Ferrero E, Malavasi F. In-tandem insight from basic science combined with clinical research: CD38 as both marker and key component of the pathogenetic network underlying chronic lymphocytic leukemia. *Blood* 2006; **108**: 1135–1144.
13 Chiorazzi N, Rai KR, Ferrarini M. Chronic lymphocytic leukemia. *N Engl J Med* 2005; **352**: 804–815.
14 Malavasi F, Deaglio S, Damle R, Cutrona G, Ferrarini M, Chiorazzi N. CD38 and chronic lymphocytic leukemia: a decade later. *Blood* 2011; **118**: 3470–3478.
15 Deaglio S, Capobianco A, Bergui L, Durig J, Morabito F, Duhrsen U *et al.* CD38 is a signaling molecule in B-cell chronic lymphocytic leukemia cells. *Blood* 2003; **102**: 2146–2155.
16 Deaglio S, Vaisitti T, Bergui L, Bonello L, Horenstein AL, Tamagnone L *et al.* CD38 and CD100 lead a network of surface receptors relaying positive signals for B-CLL growth and survival. *Blood* 2005; **105**: 3042–3050.
17 Deaglio S, Aydin S, Grand MM, Vaisitti T, Bergui L, D'Arena G *et al.* CD38/CD31 interactions activate genetic pathways leading to proliferation and migration in chronic lymphocytic leukemia cells. *Mol Med* 2010; **16**: 87–91.
18 Deaglio S, Vaisitti T, Aydin S, Bergui L, D'Arena G, Bonello L *et al.* CD38 and ZAP-70 are functionally linked and mark CLL cells with high migratory potential. *Blood* 2007; **110**: 4012–4021.
19 Vaisitti T, Aydin S, Rossi D, Cottino F, Bergui L, D'Arena G *et al.* CD38 increases CXCL12-mediated signals and homing of chronic lymphocytic leukemia cells. *Leukemia* 2010; **24**: 958–969.
20 Zucchetto A, Vaisitti T, Benedetti D, Tissino E, Bertagnolo V, Rossi D *et al.* The CD49d/CD29 complex is physically and functionally associated with CD38 in B-cell chronic lymphocytic leukemia cells. *Leukemia* 2012; **26**: 1301–1312.

21 Vaisitti T, Serra S, Pepper C, Rossi D, Laurenti L, Gaidano G *et al.* CD38 signals upregulate expression and functions of matrix metalloproteinase-9 in chronic lymphocytic leukemia cells. *Leukemia* 2013; **27**: 1177–1181.
22 Pleyer L, Egle A, Hartmann TN, Greil R. Molecular and cellular mechanisms of CLL: novel therapeutic approaches. *Nat Rev Clin Oncol* 2009; **6**: 405–418.
23 Zenz T, Mertens D, Kuppers R, Dohner H, Stilgenbauer S. From pathogenesis to treatment of chronic lymphocytic leukaemia. *Nat Rev Cancer* 2010; **10**: 37–50.
24 Deaglio S, Vaisitti T, Zucchetto A, Gattei V, Malavasi F. CD38 as a molecular compass guiding topographical decisions of chronic lymphocytic leukemia cells. *Semin Cancer Biol* 2010; **20**: 416–423.
25 Vaisitti T, Audrito V, Serra S, Bologna C, Arruga F, Brusa D *et al.* Multiple metamorphoses of CD38 from prognostic marker to disease modifier to therapeutic target in chronic lymphocytic leukemia. *Curr Top Med Chem* 2013; **13**: 2955–2964.
26 Hersher R. Companies wager high on CD38-targeting drugs for blood cancer. *Nat Med* 2012; **18**: 1446.
27 Dolgin E. Cancer's true breakthroughs. *Nat Med* 2013; **19**: 660–663.
28 Reichert JM. Antibodies to watch in 2014. *MAbs* 2013; **6**: 799–802.
29 Pearce L, Morgan L, Lin TT, Hewamana S, Matthews RJ, Deaglio S *et al.* Genetic modification of primary chronic lymphocytic leukemia cells with a lentivirus expressing CD38. *Haematologica* 2010; **95**: 514–517.
30 Bruzzone S, Moreschi I, Usai C, Guida L, Damonte G, Salis A *et al.* Abscisic acid is an endogenous cytokine in human granulocytes with cyclic ADP-ribose as second messenger. *Proc Natl Acad Sci USA* 2007; **104**: 5759–5764.
31 Bruzzone S, De Flora A, Usai C, Graeff R, Lee HC. Cyclic ADP-ribose is a second messenger in the lipopolysaccharide-stimulated proliferation of human peripheral blood mononuclear cells. *Biochem J* 2003; **375**: 395–403.
32 Zocchi E, Daga A, Usai C, Franco L, Guida L, Bruzzone S *et al.* Expression of CD38 increases intracellular calcium concentration and reduces doubling time in HeLa and 3T3 cells. *J Biol Chem* 1998; **273**: 8017–8024.
33 Deaglio S, Morra M, Mallone R, Ausiello CM, Prager E, Garbarino G *et al.* Human CD38 (ADP-ribosyl cyclase) is a counter-receptor of CD31, an Ig superfamily member. *J Immunol* 1998; **160**: 395–402.
34 Serra S, Horenstein AL, Vaisitti T, Brusa D, Rossi D, Laurenti L *et al.* CD73-generated extracellular adenosine in chronic lymphocytic leukemia creates local conditions counteracting drug-induced cell death. *Blood* 2011; **118**: 6141–6152.
35 Kellenberger E, Kuhn I, Schuber F, Muller-Steffner H. Flavonoids as inhibitors of human CD38. *Bioorg Med Chem Lett* 2011; **21**: 3939–3942.
36 Al-Abady ZN, Durante B, Moody AJ, Billington RA. Large changes in NAD levels associated with CD38 expression during HL-60 cell differentiation. *Biochem Biophys Res Commun* 2013; **442**: 51–55.
37 Escande C, Nin V, Price NL, Capellini V, Gomes AP, Barbosa MT *et al.* Flavonoid apigenin is an inhibitor of the NAD+ ase CD38: implications for cellular NAD+ metabolism, protein acetylation, and treatment of metabolic syndrome. *Diabetes* 2013; **62**: 1084–1093.
38 Budhraja A, Gao N, Zhang Z, Son YO, Cheng S, Wang X *et al.* Apigenin induces apoptosis in human leukemia cells and exhibits anti-leukemic activity *in vivo*. *Mol Cancer Ther* 2012; **11**: 132–142.
39 Munshi C, Aarhus R, Graeff R, Walseth TF, Levitt D, Lee HC. Identification of the enzymatic active site of CD38 by site-directed mutagenesis. *J Biol Chem* 2000; **275**: 21566–21571.
40 Deaglio S, Vaisitti T, Billington R, Bergui L, Omede P, Genazzani AA *et al.* CD38/CD19: a lipid raft-dependent signaling complex in human B cells. *Blood* 2007; **109**: 5390–5398.
41 Kaucka M, Plevova K, Pavlova S, Janovska P, Mishra A, Verner J *et al.* The planar cell polarity pathway drives pathogenesis of chronic lymphocytic leukemia by the regulation of B-lymphocyte migration. *Cancer Res* 2013; **73**: 1491–1501.
42 Magnone M, Bauer I, Poggi A, Mannino E, Sturla L, Brini M *et al.* NAD+ levels control Ca2+ store replenishment and mitogen-induced increase of cytosolic Ca2+ by Cyclic ADP-ribose-dependent TRPM2 channel gating in human T lymphocytes. *J Biol Chem* 2012; **287**: 21067–21081.
43 Partida-Sanchez S, Gasser A, Fliegert R, Siebrands CC, Dammermann W, Shi G *et al.* Chemotaxis of mouse bone marrow neutrophils and dendritic cells is controlled by adp-ribose, the major product generated by the CD38 enzyme reaction. *J Immunol* 2007; **179**: 7827–7839.
44 Bustelo XR. Vav proteins, adaptors and cell signaling. *Oncogene* 2001; **20**: 6372–6381.
45 Ibrahim S, Jilani I, O'Brien S, Rogers A, Manshouri T, Giles F *et al.* Clinical relevance of the expression of the CD31 ligand for CD38 in patients with B-cell chronic lymphocytic leukemia. *Cancer* 2003; **97**: 1914–1919.
46 Liu Q, Kriksunov IA, Graeff R, Munshi C, Lee HC, Hao Q. Crystal structure of human CD38 extracellular domain. *Structure* 2005; **13**: 1331–1339.
47 Bertilaccio MT, Scielzo C, Simonetti G, Ten Hacken E, Apollonio B, Ghia P *et al.* Xenograft models of chronic lymphocytic leukemia: problems, pitfalls and future directions. *Leukemia* 2013; **27**: 534–540.
48 Arnon TI, Cyster JG. Blood, sphingosine-1-phosphate and lymphocyte migration dynamics in the spleen. *Curr Top Microbiol Immunol* 2014; **378**: 107–128.
49 Lange I, Penner R, Fleig A, Beck A. Synergistic regulation of endogenous TRPM2 channels by adenine dinucleotides in primary human neutrophils. *Cell Calcium* 2008; **44**: 604–615.
50 Umar S, Malavasi F, Mehta K. Post-translational modification of CD38 protein into a high molecular weight form alters its catalytic properties. *J Biol Chem* 1996; **271**: 15922–15927.
51 Moreau C, Liu Q, Graeff R, Wagner GK, Thomas MP, Swarbrick JM *et al.* CD38 structure-based inhibitor design using the 1-cyclic inosine 5'-diphosphate ribose template. *PLoS One* 2013; **8**: e66247.
52 van der Veer MS, de Weers M, van Kessel B, Bakker JM, Wittebol S, Parren PW *et al.* Towards effective immunotherapy of myeloma: enhanced elimination of myeloma cells by combination of lenalidomide with the human CD38 monoclonal antibody daratumumab. *Haematologica* 2011; **96**: 284–290.
53 Green DJ, Orgun NN, Jones JC, Hylarides MD, Pagel JM, Hamlin DK *et al.* A preclinical model of CD38-pretargeted radioimmunotherapy for plasma cell malignancies. *Cancer Res* 2014; **74**: 1179–1189.

Supplementary Information accompanies this paper on the Leukemia website (http://www.nature.com/leu)